# Effect of Micropatterning induced Surface Hydrophobicity on Drug Release from Electrospun Cellulose Acetate Nanofibers

*Shivakalyani Adepu* [a], *Mrunalini K. Gaydhane* [b], *Manohar Kakunuri*[a], *Chandra S. Sharma*[b], *Mudrika Khandelwal*[a *], *Stephen J. Eichhorn*[c]

[a] Department of Materials Science and Metallurgical Engineering, Indian Institute of Technology, Hyderabad, Kandi, Sangareddy – 502285, Telangana, INDIA.

[b] Department of Chemical Engineering, Indian Institute of Technology, Hyderabad, Kandi-502285, Telangana INDIA.

[c] College of Engineering, Mathematics and Physical Sciences, University of Exeter, Exeter, Devon, EX4 4QF, United Kingdom.

**ABSTRACT**

Sustained release and prevention of burst release for low half-life drugs like Diclofenac sodium is crucial to prevent drug related toxicity. Electrospun nanofibers have emerged recently as potential carrier materials for controlled and sustained drug release. Here, we present a facile method to prevent burst release by tuning the surface wettability through template assisted micropatterning of drug loaded electrospun cellulose acetate (CA) nanofibers. A known amount of drug (Diclofenac sodium) was first mixed with CA and then electrospun in the form of a nanofabric. This as-spun network was hydrophilic in nature. However, when electrospinning was carried out through non-conducting templates, *viz* nylon mesh with 50 and 100μm size openings, two kinds

of hydrophobic micro-patterned CA nanofabrics were produced. *In vitro* transdermal testing of our nanofibrous mats was carried out; these tests were able to show that it would be possible to create a patch for transdermal drug release. Further our results show that with optimized micro-patterned dimensions, a zero order sustained drug release of up to 12 h may be achieved for the transdermal system when compared to non-patterned samples. This patterning caused a change in the surface wettability, to a hydrophobic surface, resulting in a controlled diffusion of the hydrophilic drug. Patterning assisted in controlling the initial burst release, which is a significant finding especially for low half-life drugs.

**Keywords:** Drug release; electrospinning; nanofibers; micro-patterning; diclofenac sodium.

## Introduction

Novel drug delivery systems are designed to deliver the bioactive agents in a controlled manner to attain therapeutic doses at a target site. The aim is to do this with minimal systemic side effects associated with the burst release and high frequency dosage for drugs that have low bioavailability.[1] Diclofenac sodium (a salt of 2-(2,6-dichloranilino) phenylacetic acid) is one such drug with a short biological half-life (of 1-2 hours) that undergoes rapid hepatic first pass metabolism following oral administration.[2] Frequent dosing is needed to maintain the therapeutic levels, and fluctuations in the drug plasma levels have adverse effects on gastric mucosa causing peptic ulcers and bleeding.[3] Diclofenac sodium (DCF) is an extensively used nonsteroidal anti-inflammatory agent for the treatment of arthritis, musculoskeletal disorders, toothache, and dysmenorrhea, as well as in catheter, heart valve linings for symptomatic relief of post-operative

pain and inflammation.[4] Transdermal patches delivering DCF for local pain management would be very useful for treating local pain. Transdermal patches based on polymeric micro/nano carrier formulations pose alternatives to conventional systems. These can sustain the release, maintain constant plasma drug levels at the target site and reduce dosing frequency leading to improved patient compliance and reduced adverse effects.[5]

The mechanism of drug release from polymeric mico/nano carrier systems is either diffusion or degradation controlled depending on the nature of the polymeric system. Drug release from polymeric systems can be controlled by varying the surface wettability of the drug carrier.[6] For hydrophilic drugs such as Diclofenac sodium, the surface of the carrier system should be hydrophobic to prevent a burst release.[6-8] The surface of a drug carrier system can be made hydrophobic by using a low surface energy coating[9] and micro/nano-patterning using techniques such as photolithography[10] and chemical vapour deposition[11]. Nevertheless, these methods often involve complex procedures to introduce functional groups and patterns and at the same time they pose issues in chemical integrity.[12]

Tuning the surface wettability through electrospinning has gained attention in recent times. Electrospinning is a facile yet effective technique which offers the benefit of fabricating polymeric nanofibers with unique micro/nano scaled topologies, which can alter surface wettability.[13] Nanofibers with patterned surfaces can be fabricated by modifying the electric field[14-15], by self-assembly[16] and by using a patterned collector.[17-19] Patterned surfaces fabricated by using collectors reported so far have used conductive templates. However, the preparation of conductive patterned surfaces requires expensive processing such as lithography.

In the current study, a non-conductive nylon mesh was used as a collector. The deposition mechanism is different for conducting and non-conducting collectors. The technique reported in

this paper is scalable due to the availability of nylon meshes with different spacings.

Recently our group has shown that the wettability of electrospun fabrics can be tuned by simply using a dielectric mesh over the collector with different opening sizes.[20] We have electrospun cellulose acetate (CA) using a nylon mesh template with three different mesh sizes (50, 100 and 200μm) to obtain a one-sided patterned surface with different wettability (a hydrophilic to hydrophobic transition). Nanofabrics collected on 50 and 100μm spacing nylon meshes showed a clear transformation to a hydrophobic behavior. Spacing greater than 200 μm essentially behaves same as non-patterned samples and exhibit hydrophilic behavior, so to control the release of the drug, 50 and 100μm mesh spacings have been chosen to tune wettability in the hydrophobic region. CA is a hydrophilic, biocompatible polymer, whose nanofibers have been extensively studied in drug delivery applications.[21] The current study aims to demonstrate the ability of micropatterned CA nanofibers to control burst release and maintain a zero order profile in comparison to non-patterned nanofibrous mats and spin coated non-fibrous thin films. Micropatterning of nanofibers allows us to control the porosity that affects the diffusion of buffer into the matrix thereby influencing drug release. For clearly demonstrating this, a comparison was made using thin films. Spin coating which is one of the most facile way to produce thin films has been chosen for this. The ability to do this is important because it would allow the production of a fibrous construct that could be used as part of a drug delivery patch.

**Materials and methods**

**Materials**

CA ($M_W$ = 29000) and Diclofenac sodium salt were purchased from Sigma Aldrich, UK. N,N-dimethylacetamide (DMAc) and acetone were purchased from Merck Specialties Private Limited, India. Nylon meshes with opening sizes of 50 and 100 µm respectively were purchased from Plastok, UK. Ultipor nylon 6,6 membrane with a pore opening of 0.3 µm was purchased from Pall India Private Ltd. Potassium chloride was purchased from HIMEDIA, while Di-sodium hydrogen orthophosphate dehydrate (analytical grade) was purchased from SDFCL, Mumbai. Potassium dihydrogen ortho-phosphate, sodium carbonate anhydrous and sodium chloride were purchased from Sisco Research Laboratories, Mumbai.

**Sample Preparation**

50 mg of Diclofenac sodium salt (DCF) was dissolved in 10 ml of mixed solvent comprising acetone and DMAc in a 2:1 (v/v) ratio. CA was slowly added and stirred for 3 h to obtain a ~13 % w/v homogenous solution. This solution was then used to make drug loaded thin films (CA-$DCF_{Thin\ film}$), non-patterned electrospun nanofiber mats (CA-$DCF_{NP}$), patterned nanofibers deposited on nylon meshes with 50µm spacings (CA-$DCF_{P\text{-}50m)}$, and 100µm spacings (CA-$DCF_{P\text{-}100m}$). The weight percentage of DCF with respect to CA in the nanofibers and thin films was 3 % (w/w).

A thin film of CA-DCF was prepared on a polymethyl methacrylate substrate for further for drug release studies. The polymer solution was deposited on the substrate prior to spinning it at 1600 rpm for 20 s to obtain a thin film of a similar thickness to the nanofiber mat at room temperature. Thickness of all the samples was measured using Vernier calipers. The spin coater used was mode: spin NXG-P1 from Apex Instruments (India).

CA-DCF solution was electrospun using equipment purchased from E-Spin Nanotech Pvt. Ltd, India. The solution was pumped out at a fixed flow rate of 10 µl/min through an 18 gauge blunt needle. The electric field was maintained at 1 kV/cm over a 10 cm spacing between the syringe and the collector plate. Three types of fibrous mats were obtained by depositing the nanofibers on nylon meshes with opening sizes of 50 and 100 µm and lastly directly onto an aluminum foil collector with no mesh; these samples were labelled CA-DCF$_{P\text{-}50m}$, CA-DCF$_{P\text{-}100m}$ and CA-DCF$_{NP}$, respectively. Another CA solution without DCF was used to make nanofibers and thin films. For the preparation of nanofibers and thin films without drug, 16 % (W/V) of cellulose acetate was dissolved in a mixed solvent system containing acetone and DMAc in 2:1 proportion. The electrospinning parameters were same as mentioned above and the patterned (CA-p50 and CA-p100) and non-patterned fibers were prepared by depositing fibers over nylon mesh with 50 µm and 100 µm mesh and aluminum foil respectively. Thin films without drugs were casted in similar fashion as mention above. Thin films and non-patterned nanofibers without the presence of the drug were named CA$_{Thin\ film}$ and CA$_{NP}$ respectively. Patterned nanofibrous mats without the presence of the drug produced with either a 50mesh or 100mesh were named as CA$_{P\text{-}50m}$ and CA$_{P\text{-}100m}$ respectively. Thickness of all these samples (without drug) as measured by Vernier caliper was same as for the samples with drug.

Further experimental details along with a schematic are provided in Supplementary Information (Figure S1).[20]

**Characterization**

The surface morphologies of electrospun fibers were assessed using a Desktop Scanning Electron Microscopy (SEM) (Model: Pro X, Phenom, Netherlands) at a 5 kV voltage, with a working distance of 10 mm. Average fiber diameter was calculated from SEM images using Image J software considering 50 fibers into consideration for each images. For a given sample, at least two SEM images were considered for more precise measurement of average fiber diameter. Electrospun CA-DCF fibers, CA nanofibrous mats and DCF powder were characterized using a Fourier Transform Infrared (FTIR) spectrometer (Model: Alpha-P, Bruker Corporation, USA) working in an attenuated total reflection (ATR) mode in the wavenumber range of 4000 and 500 $cm^{-1}$. The wettability of the all nanofiber as well as thin film samples with and without drug were studied in triplicate using a sessile drop method with a goniometer (Rame-Hart, USA; Model: 290-F4). A 3 µl deionized (DI) water droplet, ~2 mm in diameter, was used for contact angle measurements. The surface area of the nanofibers and thin films were calculated using multi-point Brunauer-Emmett-Teller (BET) analysis. $N_2$ physisorption was determined using a Micromeritics ASAP 2020 physisorption analyzer (USA). All samples of 100 mg mass were degassed at 80 °C for 1-2 h in a nitrogen atmosphere. The BET and porosity results are presented in Supplementary Information (Table 1S). XRD patterns were obtained using a Bruker X-ray diffractometer with nickel-filtered Cu K$\alpha$ radiation, a 2θ step size of 0.02°◦ from 5 to 60°, and a dwell time of 3s. DSC analysis of all samples was carried out using a simultaneous thermal analyzer NETZSCH STA 449 F3 Jupiter instrument. Samples were weighed directly on aluminium pans and scanned between 30-300 °C at a heating rate of 10°C/min in an Argon atmosphere at a 50ml/min flow rate. Further, we measured the drug entrapment efficiency in drug load nanofibers (patterned and non-patterned) and thin film samples. Drug entrapment efficiency is defined as the weight ratio of amount of drug loaded in the nanofiber to the total amount of drug added in the feed solution. To

determine the entrapment efficiency of drug loaded nanofibers and thin film, the samples of predetermined mass were sonicated in 20 mL of phosphate buffered saline (PBS) pH~5.5 for 15 minutes, with pulse duration of 2 seconds-"On" and 3 seconds "Off". The release medium was then centrifuged for 5 minutes at 2000g to bring down the nanofiber and thin film fragments. The total amount of drug released in PBS was estimated by UV-Vis analysis of the resultant release medium and then correlating the absorbance values with standard plot of Diclofenac sodium.

Drug entrapment efficiency was calculated by following equation:

Entrapment efficiency = (Total mass of drug released from nanofiber/Mass of total drug added) ×100 (1)

***In vitro* transdermal drug release study**

A modified Franz diffusion cell was used for the transdermal drug release studies. It consisted of an upper donor chamber and a lower receiver chamber. In between these two chambers, a multipore membrane of ~0.3 μm pore size was placed (which mimics the porosity of skin) followed by a test sample with the patterned side facing towards the donor chamber. PBS of pH~5.5 was used for the release studies to match the pH of skin. The donor chamber was filled with 20ml of PBS pH ~ 5.5 buffer and the entire set up was kept at 37 ± 1 °C with a 50 rpm rotation. 3 ml aliquots were collected at specified time intervals for measurements and replaced with the fresh buffer to maintain sink conditions. All the experiments were conducted in triplicate. The amount of drug released was estimated from the UV absorbance (SATHYAM LI-2700 double beam UV-Visible spectrophotometer) of the removed aliquots and a predetermined calibration curve. A schematic of the transdermal release study is presented in Figure S2 (Supplementary information).

A calibration curve of DCF in PBS 5.5 was determined and the $R^2$ value was found to be 0.99 (Figure.7).

## Results and Discussion

### Surface morphology and wettability

Figure. 1 reports typical SEM and contact angle (with buffer PBS pH~5.5) images of drug loaded non-patterned and micro-patterned CA nanofibers mats. Figure 2 reports typical SEM and contact angle (with buffer PBS pH~5.5) images of non-patterned and micro-patterned CA nanofibers mats without the presence of the drug. From SEM analysis we could observe the uniformly distributed fiber mat with smooth, slender and beadless nanofibers in all the samples. The SEM analysis of non-patterned samples showed random and uniform deposition of nanofibers while in case of patterned nanofibers we could vividly observe the patterns showing the deposition along the meshlines. Random deposition of fibers as observed for CA-$DCF_{NP}$ (Fig. 1a) exhibits a water contact angle of 33.9±0.5° (hydrophilic). During template-assisted electrospinning, initially for about 10 min, nanofibers deposit over the nylon threads in the mesh. However, later on in the process the fibers deposit randomly due to a decay in the dielectric mesh effect.[20] This preferential deposition over the mesh lines followed by a random deposition results in micro-patterned nanofibrous mats with two surfaces with different wettability. After peeling (Figure S1), the surface towards the nylon mesh exhibits hydrophobic properties (Figures 1b and 1c) with contact angles of 134.6±0.1° and 117.6±0.1° for CA-$DCF_{P\text{-}50m}$ and CA-$DCF_{P\text{-}100m}$, respectively. The surface facing the syringe exhibits hydrophilic properties, similar to CA-$DCF_{NP}$. The patterned samples, CA-$DCF_{P\text{-}50m}$ and CA-$DCF_{P\text{-}100m}$, exhibit cup-like non-continuous air traps which suspend the water droplet, leading to an increase in the hydrophobic behavior. For CA Nanofibers

without drug, contact angle for $CA_{NP}$ was found to be 29.7±0.1°. The surface towards the nylon mesh, after being peeled, exhibits hydrophobic behaviour (Figure. 2) with contact angles of $129.8\pm0.1^0$ and $137.8\pm0.1^0$ for $CA_{P\text{-}100m}$ and $CA_{P\text{-}50m}$, respectively. The surface towards the syringe exhibits hydrophilic behaviour, similar to $CA_{NP}$ (29.7±0.1°). The contact angle values for $CA_{Thin\ film}$ and $CA\text{-}DCF_{Thin\ film}$, were found to be 73.2±0.2° and 71.0±0.1°, respectively (Figure.3.) These are indicative of intermediate hydrophilic-hydrophobic properties. The effect of micro-patterning on electrospun nanofibers in terms of how it effects the water contact angle is explained in our recent work.[20] In summary, we have demonstrated the fabrication of micropatterned nanofiber mats with tunable wettability using template based electrospinning. Patterned nanofiber mats were shown to possess hydrophobic behavior due to a non-wetting capillary pressure which in turn is due to air trapped in the non-communicating air gaps. Briefly, for micropatterned samples capillary pressure plays an important role in surface wettability. Air trapped in cup type structures in micropatterned mats possess a non-wetting capillary pressure. This non-wetting pressure increases with decreasing spacing between features and results in a higher contact angle for $CA\text{-}DCF_{P\text{-}50}$ and $CA_{P\text{-}50}$ when compared to $CA\text{-}DCF_{P\text{-}100}$ and $CA_{P\text{-}100}$.

Here, in this study we have used patterned nanofiber mats as drug carriers and investigated the effect of wettability of mats on drug release. Average fiber diameters as calculated from SEM images using Image J software are listed in Table 1. Drug entrapment efficiency was calculated by following equation and the results are given in Table 1.

Entrapment efficiency = (Total mass of drug released from nanofiber/Mass of total drug added) ×100 (1)

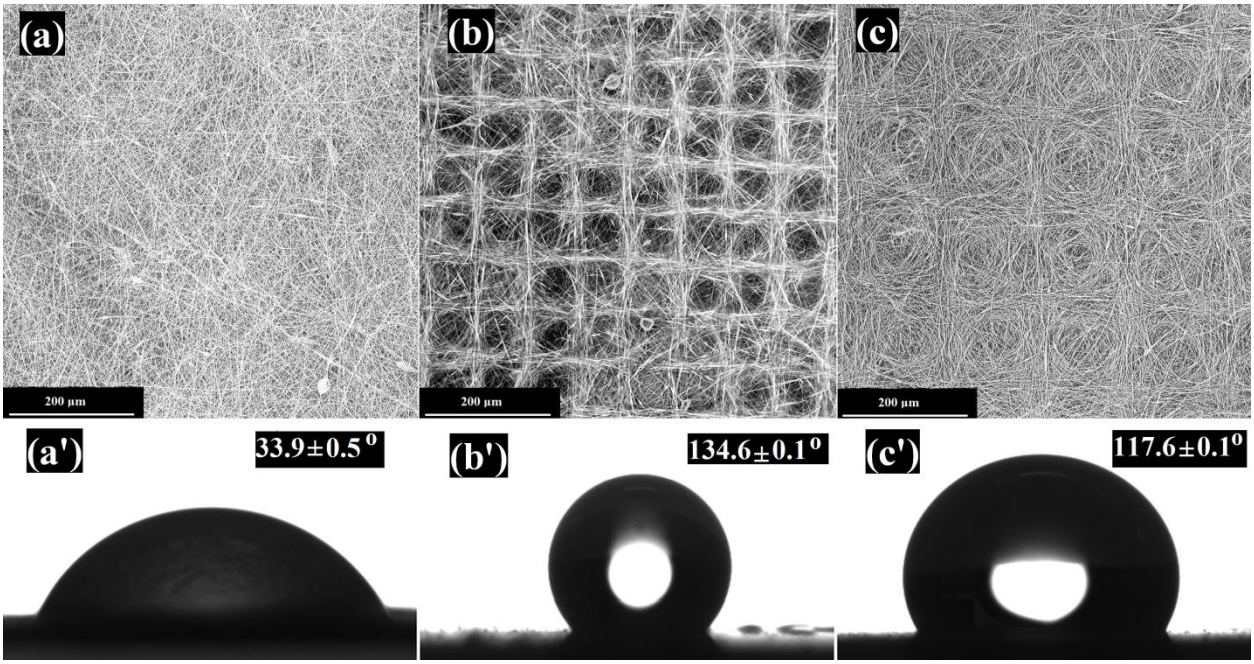


**Figure.1.** SEM and contact angle (with PBS pH ~5.5) images for (a) & (a') $CA\text{-}DCF_{NP}$, (b) & (b') $CA\text{-}DCF_{P\text{-}50m}$ and (c) & (c') $CA\text{-}DCF_{P\text{-}100m}$

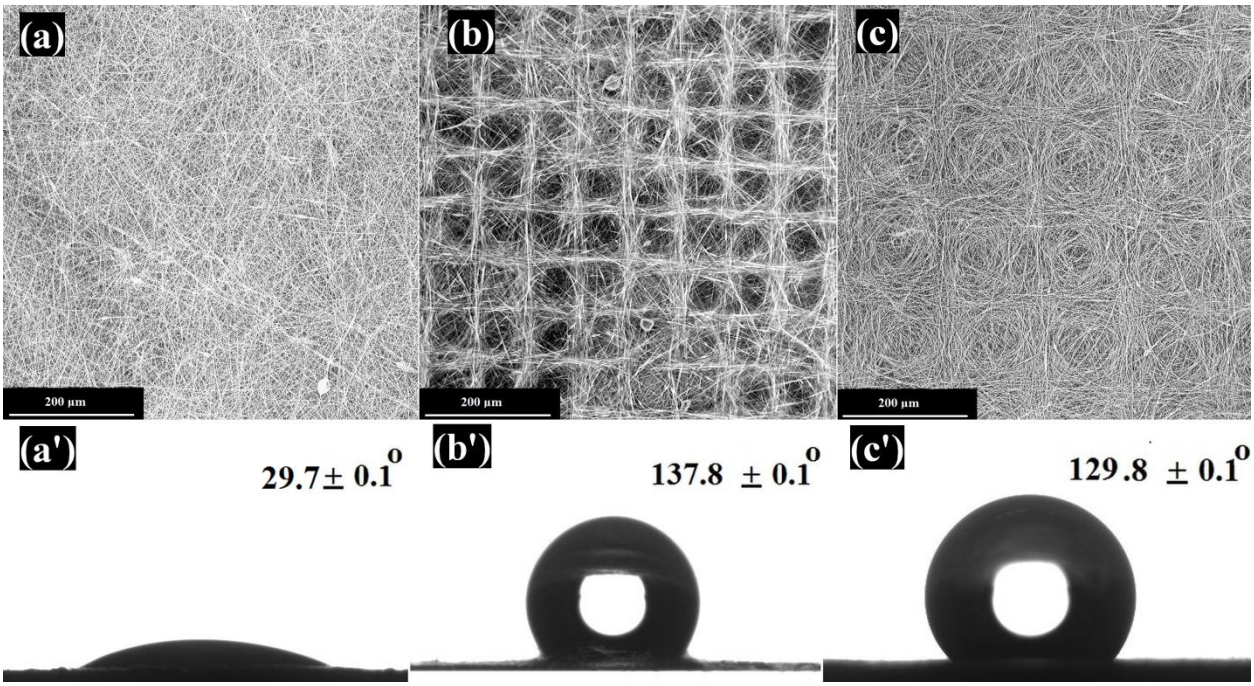

**Figure.2.** SEM and contact angle images of (a) & (a') $CA_{NP}$, (b) & (b') $CA_{P\text{-}50m}$ and (c) & (c') $CA_{P\text{-}100m}$

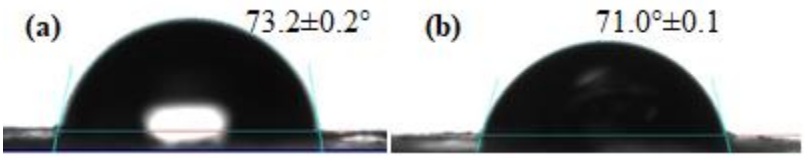


**Figure.3.** Contact angle images of (a) $CA_{Thin\ film}$, (b) CA-$DCF_{Thin\ film}$

**Table.1** Average fiber diameter and drug entrapment efficiency

| Sample | Average fiber diameter (nm) | Drug entrapment efficiency (%) |
|---|---|---|
| **$CA_{NP}$** | 361±90 | - |
| **$CA_{P\text{-}50m}$** | 362±91 | - |
| **$CA_{P\text{-}100m}$** | 368±84 | - |
| **CA-$DCF_{NP}$** | 351±98 | 97±0.74 |
| **CA-$DCF_{P\text{-}50m}$** | 349±95 | 99±1.74 |
| **CA-$DCF_{P\text{-}100m}$** | 349±95 | 98±1.23 |
| **CA-$DCF_{Thin\ film}$** | - | 56±1.85 |

**FTIR Analysis**

FTIR analysis was performed for $CA_{NP}$, DCF powder and CA-$DCF_{NP}$ in order to understand the drug polymer interaction. FTIR result confirms the successful incorporation of DCF in CA nanofibers without any chemical interactions (Figure 4).

The IR spectra of $CA_{NP}$ (Figure 4a) have acetate group vibrations located at ~599 $cm^{-1}$ ($_{O\text{-}C\text{-}O}$ bend of ester) ~895 $cm^{-1}$ ($\delta_{CH2}$), ~1047 $cm^{-1}$ ($\upsilon_{C\text{-}O\text{-}C}$), ~1236 $cm^{-1}$ ($\upsilon_{C\text{-}O\text{-}C}$), ~1373 $cm^{-1}$ ($\upsilon_{C\text{-}CH3}$), 1624

$cm^{-1}$ (alkenyl $\upsilon_{C=C}$ stretching) ~1754 $cm^{-1}$ ($\upsilon_{CO}$), ~2949 $cm^{-1}$ ($\upsilon_{C-CH3}$) and ~3477 ($\upsilon_{OH}$) [24]. The IR spectrum of DCF powder (Figure 4b) has a characteristic vibration located around ~746-778 $cm^{-1}$ due to the substituted phenyl group stretch, $\upsilon_{C=C}$ vibrations from 1400 to 1570 $cm^{-1}$, aromatic =CH stretch at 2962-3079 $cm^{-1}$, phenolic stretch at 3254 $cm^{-1}$, characteristic primary amine stretch at 3390 $cm^{-1}$ along with a small peak for $\upsilon_{C-Cl}$ located at ~558 $cm^{-1}$ [22-23]. The IR spectra of DCF loaded CA nanofibers (as shown in Figure 4c) has shown all the characteristic peaks from CA. For instance, we could observe same peaks at 599 $cm^{-1}$, 895 $cm^{-1}$ 1047 $cm^{-1}$,1236 $cm^{-1}$, and 1754 $cm^{-1}$ while peak shifts to higher wavenumber means lowering of bond length were recorded at 1377 $cm^{-1}$ and 1632 $cm^{-1}$ corresponding to that at 1624 $cm^{-1}$ and 1373 $cm^{-1}$. The successful incorporation of drug is prominently shown through aromatic C-H bending at 786 $cm^{-1}$, amide C=O stretch at 1632 $cm^{-1}$, and incorporation of primary amines at 3500 $cm^{-1}$ which suggests the existence of hydrogen bonding between the drug and the CA fibers. No new peaks and no significant shift in the peak position were observed for the CA-$DCF_{NP}$ samples, when compared to pristine DCF and $CA_{NP}$. This further shows the stability of the drug while loaded in CA nanofibers. Further, as the chemical composition including the drug loading, solution concentration and parameters for electrospinning and spin coating were the same for both patterned nanofibers (CA-DCF-p50 and CA-DCF-p100) and CA-DCF $_{Thin\ film}$, no separate spectra was recorded for these samples.

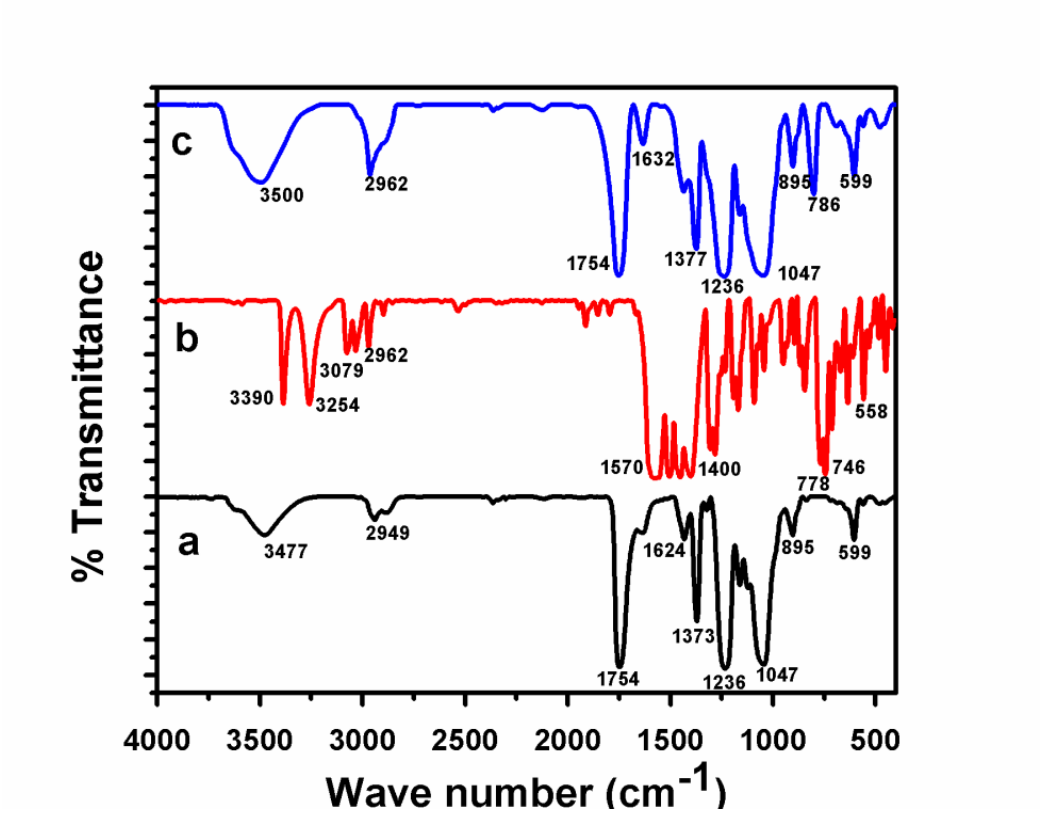


**Figure. 4.** Typical FTIR spectra for (a) $CA_{NP}$, (b) DCF powder and (c) $CA\text{-}DCF_{NP}$

**DSC Analysis**

The determination of the physical state of the drug in the nanofibers is essential to achieve the desired drug release profiles. In the present study, DSC and XRD analysis was undertaken to determine the physical status of the components of the composite nanofibers.

DSC analysis was performed for DCF powder, $CA_{NP}$, drug loaded CA nanofibers ($CA\text{-}DCF_{NP}$, $CA\text{-}DCF_{P\text{-}50m}$, $CA\text{-}DCF_{P\text{-}100m}$) and the drug loaded thin film ($CA\text{-}DCF_{Thin\ film}$) samples. An overlay of the DSC thermograms is presented in Figure.5. The thermogram for $CA_{NP}$ shows a broad endothermic event located at around 60-100°C which is attributed to the dehydration of the polymer. A broad low endothermic is observed around 215-230 °C, which is attributed to the

melting ($T_m$) temperature. Absence of clear melting endothermic peak in thermogram of CA indicates the amorphous nature of $CA_{NP}$.

The DSC thermogram of pure DCF exhibited a transition peak at 54°C as a result of some structural rearrangements (polymorphic transformations). A sharp peak at 274°C corresponds to the melting temperature of DCF, which suggests that DCF is crystalline in nature. Peaks around 300°C may be attributed to the initiation of oxidative degradation of the drug.

The thermograms of CA-$DCF_{Thin\ film}$, CA-$DCF_{NP}$, CA-$DCF_{P\text{-}50m}$ and CA-$DCF_{P\text{-}100m}$ shows a broad endothermic event located at around 60-100°C which is attributed to the dehydration of the polymer. They also exhibited a weak and broad transition ranging from 215 to 230 °C due to the melting temperature ($T_m$) of CA, suggesting that CA nanofibers and thin film samples retained amorphous nature even after drug loading. The CA-$DCF_{Thin\ film,}$ CA-$DCF_{NP}$, CA-$DCF_{P\text{-}50m}$ and CA-$DCF_{P\text{-}100m}$ samples did not show any sharp melting peak as in case of pure DCF, suggesting that the DCF present in the composite nanofibers was in an amorphous state, having lost its original crystalline state. As patterning does not alter the melting point of DCF loaded CA nanofibers, similar results were observed for the entire drug loaded nanofibers.

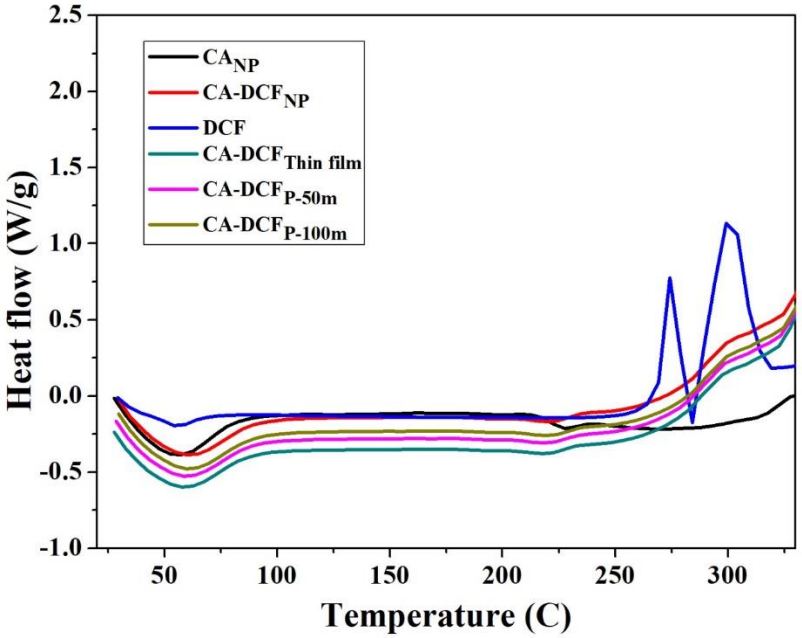


**Figure.5.** Typical DSC thermograms of $CA_{NP}$, DCF powder, drug loaded CA nanofibers (CA-$DCF_{NP}$, CA-$DCF_{P\text{-}50m,}$ CA-$DCF_{P\text{-}100m}$) and thin film (CA-$DCF_{Thin\ film}$) samples.

**XRD Analysis**

The presence of numerous distinct peaks in the XRD patterns of pure DCF powder indicates that DCF is a crystalline material with characteristic diffraction peaks (Figure 6a). $CA_{NP}$ did not exhibit any distinct sharp peaks and a broad 'hump' was observed in the XRD pattern (Figure 6b), indicating the amorphous nature of CA. Irrespective of patterning, there are no peaks pertaining to crystalline DCF are detectable in the XRD patterns of all the three DCF-loaded CA nanofibers (Figure 6c-e), indicating that the entire DCF loaded in the CA nanofibers no longer retained its crystalline nature, but had been totally transformed into an amorphous state.

The thin film sample (CA-$DCF_{Thin\ film}$) also exhibits a characteristic 'hump' attributed to an amorphous state to the material (Figure. 6f).

The XRD results are in agreement with the findings from DSC, likewise validating that DCF molecules were well distributed in the CA nanofiber matrix and were present in a complex manner in which the original structure of the pure, crystalline DCF material was lost.

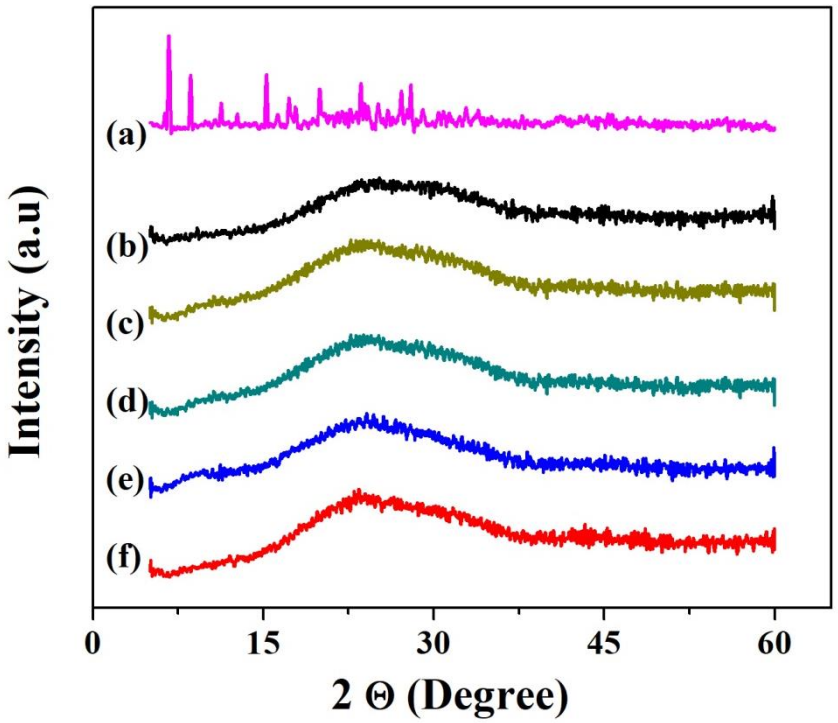


**Figure 6.** Typical XRD patterns of (a) DCF, (b) $CA_{NP}$, (c) CA-$DCF_{NP}$, (d) CA-$DCF_{P\text{-}50m}$, (e) CA-$DCF_{P\text{-}100m,}$ (f) CA-$DCF_{Thin\ film}$ samples.

**In-vitro transdermal drug release**

A calibration curve of DCF in PBS pH~5.5 is presented in figure.7. *In vitro* transdermal release profiles of all the samples are presented in Figure 8. The cumulative percentage drug releases after 48 h for CA-$DCF_{P\text{-}50m}$, CA-$DCF_{P\text{-}100m}$, and CA-$DCF_{NP}$ were found to be 99.5, 98.6 and 97.8, respectively (Figure 8a). Only 32.5% of the drug was released in the case of CA-$DCF_{Thin\ film}$ by the end of 48h due to the low porosity and the poor penetration of the buffer solution into the material. As summarized in Table 1S, the porosities of CA-$DCF_{P\text{-}50m}$ and CA-$DCF_{P\text{-}100m}$ were

found to be close to 0.986 and 0.982, while for CA-DCF$_{NP}$ and CA-DCF $_{Thin\ film}$, values of 0.925 and 0.356 were obtained respectively.

The cumulative percentage drug releases after first 12h for CA-DCF$_{P\text{-}50m}$, CA-DCF$_{P\text{-}100m}$, and CA-DCF$_{NP}$ were found to be 52.7, 72.6 and 76.5, respectively (Figure. 8b). Only 14.5% of the drug was released in case of CA-DCF $_{Thin\ film}$ by the end of 12h due to the low porosity and the poor penetration of the buffer solution into the material. Burst release was observed in CA-DCF$_{NP}$; whereas a gradual incremental profile was observed with 100M. A completely linear profile was observed for the CA-DCF$_{P\text{-}50m}$ sample; <15% release was observed in CA-DCF $_{Thin\ film}$. A zero order release profile (where amount of drug release at each time point is same) was observed after 12h for the CA-DCF$_{P\text{-}50m}$ sample, 3h for the CA-DCF$_{P\text{-}100m}$ sample, and 1h for the CA-DCF$_{NP}$ sample.

It is evident from the above result that drug release in transdermal patches depends upon the surface wettability.[17] When the contact angle of the surface in touch with the buffer is small (hydrophilic) there is an enhanced wetting, thereby increasing the extent of matrix diffusion and swelling. This assists in an increased release of the drug. In this case, patterning induced hydrophobicity results in increased contact angles of 134.6±0.1° and 117.6±0.1° for CA-DCF$_{P\text{-}50m}$ and CA-DCF$_{P\text{-}100m}$ respectively when compared to CA-DCF$_{NP}$ (33.9±0.5°). Due to the formation of air pockets at the interface of the patterned surface and the release medium, the effective area in contact with the medium is reduced, thus preventing burst release. In CA-DCF$_{Thin\ film}$, even though the effective surface area in contact with the medium may be high, a lower porosity causes poor penetration of the buffer, and therefore the total cumulative release is reduced. There is a significant difference in the amount of drug released was observed with CA-DCF$_{P\text{-}50m}$ for CA-DCF$_{P\text{-}100m.}$ Even though both are patterned nanfibrous mats, CA-DCF$_{P\text{-}100m}$ was unable to sustain zero order release for

much longer time when compared to CA-DCF$_{P\text{-}50m}$. This may be due to the formation and retention of air pockets at the interface of CA-DCF$_{P\text{-}50m}$ and the buffer. The CA-DCF$_{P\text{-}100m}$ sample was however unable to retain air pockets for long durations as its contact angle is lower than CA-DCF$_{P\text{-}50m.}$ When the nanofibrous mat becomes more wetted by the buffer solution, the surface area of the mat in contact with the buffer increases. The drug then diffuses into the buffer more rapidly due to its hydrophilicity. Comparing the CA-DCF$_{P\text{-}50m}$ and CA-DCF$_{P\text{-}100m}$ samples, the latter has a lower contact angle with the buffer, and a greater surface area in contact with the buffer. Therefore, the amount of drug released is expected to be more than for CA-DCF$_{P\text{-}50m.}$

After 24 h, the release profiles of all the three (CA-DCF$_{NP,}$ CA-DCF$_{P\text{-}50m}$ and CA-DCF$_{P\text{-}100m}$) samples were found to be similar. As time progresses, the trapped air is released and the interface becomes completely wetted out. This leads to the diminishing of any surface effects on drug release translating to similar release profiles for patterned as well as non-patterned samples after 24 h.[8, 25]

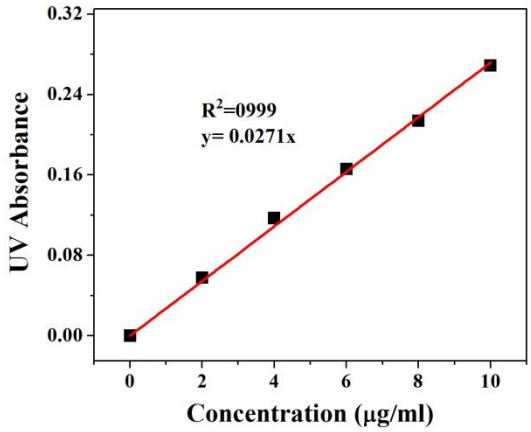


**Figure.7.** Calibration curve of DCF in PBS pH~5.5

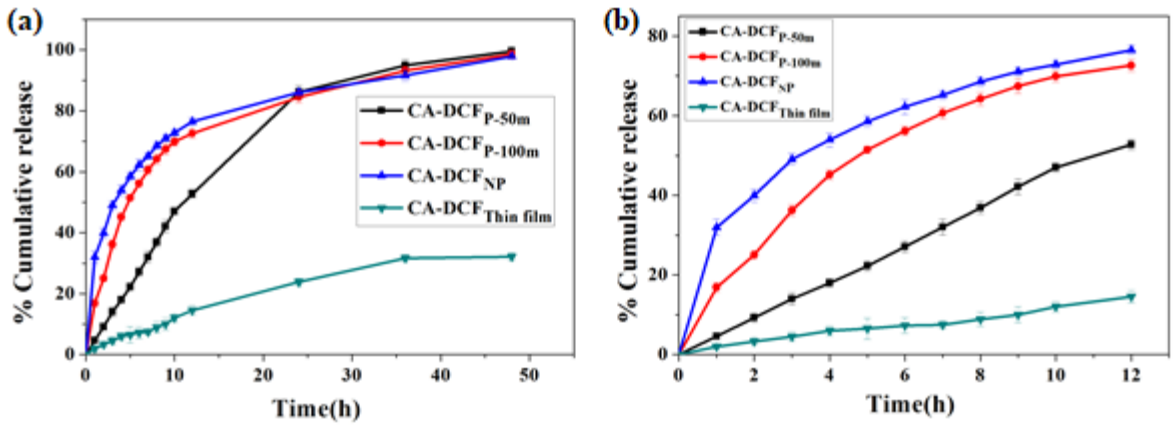


**Figure.8.** Cumulative *in vitro* transdermal release profiles of DCF from ($CA\text{-}DCF_{NP}$ , $CA\text{-}DCF_{P\text{-}50m}$ , $CA\text{-}DCF_{P\text{-}100m}$, and $CA\text{-}DCF_{Thin\ film}$,) in PBS pH~5.5 for (a) 48h (b) first 12h

After an initial phase of drug release from the surface, the drug tends to release from the bulk, where porosity plays an important role in the process. The swelling of the mat and the diffusion of the drug from the polymeric matrix increases with an increase in porosity. As $CA\text{-}DCF_{P\text{-}50m}$ has the highest porosity amongst the three samples, slightly higher cumulative release is observed after 24h. However, given enough time, all samples exhibit a similar cumulative release.

**Mathematical modeling of release kinetics**

Well-established mathematical models are available in the literature to understand and infer drug release mechanisms. The drug release profile data were fitted with various existing mathematical models in order to better understand the drug release mechanisms. These models were zero order, first order, Higuchi, Hixson-Crowell and Korsmeyer-Peppas.

In the transdermal release studies, a zero order profile was observed for first 12, 3 and 1 h of release with $CA\text{-}DCF_{P\text{-}50m}$, $CA\text{-}DCF_{P\text{-}100m}$ and $CA\text{-}DCF_{NP}$ samples respectively as seen in Figure 9. ($R^2$ values obtained from the regressions are included in Table.2). This implies that the drug release rate is constant and independent of concentration in these regions. Slope of the linear fitted curves

gives information on the drug release rate. Slopes of CA-$DCF_{NP,}$ CA-$DCF_{P\text{-}50m}$ and CA-$DCF_{P\text{-}100m}$ were found to be 32.3, 4.5 and 11.7 % $h^{-1}$, respectively; the release rate is therefore highest for CA-$DCF_{NP}$ amongst the three samples.

The rate-limiting step for water soluble drug (DCF) loaded in water insoluble and non-erodible polymeric systems (CA Nanofibers) is the diffusion through typically a water-insoluble barrier. DCF loaded CA Nanofibers is matrix-based system, where the drug is uniformly distributed in the polymeric matrix and water permeation leads to swelling of the matrix causing pores. In order for effective diffusion of drug molecules to occur, the pore size of the swelled matrix must greatly exceed the size of the hydrophilic drug molecule. Extent of wetting of the nanofibrous mat at interface with buffer determines the degree of diffusion of buffer and swelling of matrix. In case of CA-$DCF_{P\text{-}50m,}$ air trapped at the interface reduced the extent of wetting and diffusion of buffer, thereby reducing the burst release of drug at initial phase. Therefore, zero order profile was observed for 12h in case of CA-$DCF_{P\text{-}50m.}$ Due to the absence of such mechanism in rest of the samples, zero order profile was short-lived.

After this zero order profile behavior, CA-$DCF_{P\text{-}50m}$ followed a Hixson-Crowell model till 48h. According to Hixson-Crowell model, a plot of cube root of the unreleased fraction of the drug versus time will be linear if the equilibrium conditions are not reached and if the geometrical shape of the pharmaceutical dosage form diminishes proportionally over time.

As described earlier, after first 12h, release rate was increased in case of CA-$DCF_{P\text{-}50m}$ when compared to CA-$DCF_{NP}$ and CA-$DCF_{P\text{-}100m}$ pertaining to highest porosity of the matrix which assisted in enhanced penetration of buffer. As buffer penetrates and swelling takes place, a transformation of polymer from a glassy to rubbery state occurs and the dimension of the matrix increases slightly. This transformation of state essentially creates a gel layer of rubbery region for

the drug to diffuse, in which the drug diffusivity increases significantly. As a result, during the swelling, two different states, namely the glassy core and rubbery surface (gel layer), exist in the polymer matrix. At this point, two moving fronts exist, namely the glassy-rubbery front (R) and the rubbery–solvent front (S). Initially during swelling, front R moves inwards, whereas front S moves outward. As soon as the polymer at interface S achieve thermodynamic equilibrium with the surrounding medium, drug at interface S dissolves and create pores and, thus, front S moves inwards. Both fronts move inwards till the front R diminishes as the glassy core wanes. Later, only the rubbery region exists and drug dissolution at interface S eventually controls the shrinking process. This indicates that the drug release rate in CA-DCF$_{P\text{-}50m}$ is limited by the drug particles dissolution rate and not by the diffusion that occurs through the polymeric matrix. This model has been used to describe the role of surface volume relationships on release profile keeping in mind the diminishing surface of the drug particles during the dissolution[26, 27].

After zero order profile, CA-DCF$_{NP}$ and CA-DCF$_{P\text{-}100m}$ exhibited first order release kinetics till 48h, which is matrix diffusion controlled and concentration gradient dependent. Drug release rate was higher for CA-DCF$_{NP}$ and CA-DCF$_{P\text{-}100m}$ when compared to CA-DCF$_{P\text{-}50m}$ during first 12h, but, decreased later. About 75% of drug release was observed within first 12h for CA-DCF$_{NP}$ and CA-DCF$_{P\text{-}100m,}$ less amount of drug was available in matrix for further release. As per first order fitting, drug release rate is proportional to the amount of drug remaining to release from the nanofibrous mat[26, 27]. Therefore, release rate was decreased after 12h.

As the rate of diffusion depends on the surface wettability and therefore is due to differences in contact angles. The three samples show very different release profiles. In the first order phase, drug releases from the bulk of the porous matrix, where concentration gradient and distance of matrix to fresh buffer affects the release.

The two main advantages of the CA-DCF$_{P\text{-}50m}$ patterned mats are – control over burst release, and the presence of a zero order profile up to 12h. As discussed earlier, this kind of a patterned release system could be useful for low half-life drugs. The patterning would prevent burst release and extend the release period for these materials.

Release study of electrospun nanofibers loaded with Diclofenac sodium was extensively studied by complete immersion test[26-31] including transdermal release as well. However in these studies, up to 50% of drug release was observed in complete immersion test and >25% of the drug release was observed in transdermal first 2h[28-33]. There was minimal or no control over burst release. None of these studies achieved 12h zero order release profile with a controlled release profile till 48h[28-33]. In the present study, non-patterned electrospun fibers were unable to achieve longer zero order profile much similar to that of earlier studies. However altering the surface wettability of electrospun nanofibers through template based micropatterning played pivotal role in achieving zero order profile. Even though CA-DCF$_{P\text{-}100m}$ is patterned, it was unable to achieve prolonged zero order profile. Hence, close control of the mesh spacing is crucial to obtain desired results.

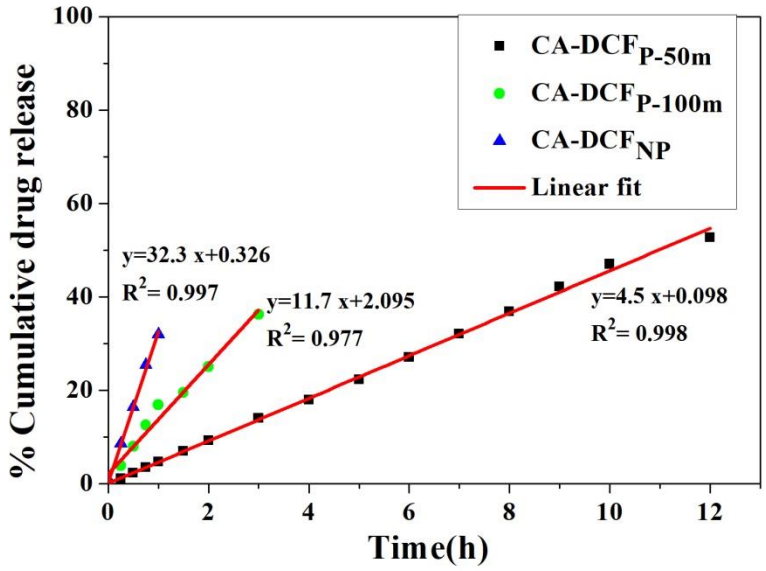

**Figure.9.** Zero order fitting curves for CA-DCF$_{NP}$ (first 1h), CA-DCF$_{P\text{-}100m}$ (first 3h), CA-DCF$_{P\text{-}50m}$ (first 12h) samples.

**Table.2** Zero order release region for transdermal study

| **Sample** | **Time point till which release followed zero order (h)** | **$R^2$ value for zero order fitting** | **Slope (% $h^{-1}$)** |
|---|---|---|---|
| **CA-DCF$_{NP}$** | First 1h | 0.997 | 32.3 |
| **CA-DCF$_{P\text{-}50m}$** | First 12h | 0.977 | 4.5 |
| **CA-DCF$_{P\text{-}100m}$** | First 3h | 0.998 | 11.7 |

## Conclusions

The effect of a variation in surface wettability of drug embedded nanofibrous and patterned polymeric matrix on the transdermal release of a hydrophilic drug (Diclofenac sodium) has been successfully investigated. The variation in wettability was obtained by tuning the air-liquid interface of a patterned mat, by changing the template mesh dimensions used in an electrospinning process. A much higher drug release was obtained for nanofibrous mats (patterned and non-patterned) compared to a thin film of the same thickness obtained by spin coating. This was thought to be due to an increased solid-liquid interface. The patterned side of the networks showed controlled release due to a minimized solid-liquid interface compared to a non-patterned electrospun mat.Patterned mats obtained using 50 μm mesh demonstrated zero order release up to 12 h, as compared to 3 h and 1 h for a 100 μm mesh and a non-patterned mat respectively. This is due to higher contact angle for the 50 μm mesh sample, which reduces the contact area and hence

controls the release. This suggests further fabrication of multi-layered hydrophobic mats would be required to obtain a zero order profile for an extended period of time.

Further, several other high potent drugs with low half-life could be loaded in micro-patterned nanofibrous mats to achieve zero order profile for transdermal applications. Multiple layers of micropatterned nanofibrous mats could be stacked together to control the drug release from the surface as well as from the bulk. Such multilayer patterning could control the burst release in implantable systems and depot formulations as well. By this way, they may provide a zero order profile for prolonged time, even after 12h.

## AUTHOR INFORMATION

Corresponding Author

* Mudrika Khandelwal, Department of Materials science and Metallurgical Engineering, Indian Institute of Technology, Hyderabad, Kandi-502285, Telangana (INDIA); Phone:(+91) 40-2301 7118; Email: mudrika@iith.ac.in

### Author Contributions

The manuscript was written through contributions of all authors. All authors have given approval to the final version of the manuscript.

### Funding Sources

Authors acknowledge the support of DST-UKERI grant (IND/CONT/E/14-15/370 & DST/INT/UK/P-92/14).

### Acknowledgements

Authors acknowledge the Indian Institute of Technology, Hyderabad for providing necessary research infrastructure to carry out this work. The authors also acknowledge Dr. Balaji Padya, Centre for Carbon Materials, ARCI for his help to perform DSC analysis.CSS acknowledges DST INSPIRE Faculty award research grant for electrospinning facility.

## REFERENCES

1. Hoffman, A. S., The origins and evolution of "controlled" drug delivery systems. *Journal of Controlled Release* **2008,** *132* (3), 153-163.

2. Willis, J.; Kendall, M.; Flinn, R.; Thornhill, D.; Welling, P., The pharmacokinetics of diclofenac sodium following intravenous and oral administration. *European Journal of Clinical Pharmacology* **1979,** *16* (6), 405-410.

3. Small, R., Diclofenac sodium. *Clinical Pharmacy* **1989,** *8* (8), 545-558.

4. Campbell, W.; Kendrick, R., Intravenous diclofenac sodium does its administration before operation suppress postoperative pain? *Anaesthesia* **1990,** *45* (9), 763-766.

5. Goonoo, N.; Bhaw-Luximon, A.; Jhurry, D., Drug loading and release from electrospun biodegradable nanofibers. *Journal of Biomedical Nanotechnology* **2014,** *10* (9), 2173-2199.

6. Zhang, Y.; Cun, D.; Kong, X.; Fang, L., Design and evaluation of a novel transdermal patch containing diclofenac and teriflunomide for rheumatoid arthritis therapy. *Asian Journal of Pharmaceutical Sciences* **2014,** *9* (5), 251-259.

7. Reza, M. S.; Quadir, M. A.; Haider, S. S., Comparative evaluation of plastic, hydrophobic and hydrophilic polymers as matrices for controlled-release drug delivery. *Journal of Pharmacy & Pharmaceutical Sciences* **2003,** *6* (2), 282-91.

8. Yohe, S. T.; Colson, Y. L.; Grinstaff, M. W., Superhydrophobic materials for tunable drug release: using displacement of air to control delivery rates. *Journal of the American Chemical Society* **2012,** *134* (4), 2016-2019.

9. Zhai, L.; Berg, M. C.; Cebeci, F. C.; Kim, Y.; Milwid, J. M.; Rubner, M. F.; Cohen, R. E., Patterned superhydrophobic surfaces: toward a synthetic mimic of the Namib Desert beetle. *Nano Letters* **2006,** *6* (6), 1213-1217.

10. Champion, J. A.; Katare, Y. K.; Mitragotri, S., Particle shape: a new design parameter for micro-and nanoscale drug delivery carriers. *Journal of Controlled Release* **2007,** *121* (1), 3-9.

11. Im, S. G.; Kusters, D.; Choi, W.; Baxamusa, S. H.; Van de Sanden, M.; Gleason, K. K., Conformal coverage of poly (3, 4-ethylenedioxythiophene) films with tunable nanoporosity via oxidative chemical vapor deposition. *ACS Nano* **2008,** *2* (9), 1959-1967.

12. Ramakrishna, S.; Fujihara, K.; Teo, W.-E.; Lim, T.-C.; Ma, Z., *An introduction to electrospinning and nanofibers*. World Scientific: **2005**; Vol. 90.

13. Wu, H.; Zhang, R.; Sun, Y.; Lin, D.; Sun, Z.; Pan, W.; Downs, P., Biomimetic nanofiber patterns with controlled wettability. *Soft Matter* **2008,** *4* (12), 2429-2433.

14. Li, D.; Wang, Y.; Xia, Y., Electrospinning nanofibers as uniaxially aligned arrays and layer-by-layer stacked films. *Advanced Materials* **2004,** *16* (4), 361-366.

15. Li, D.; Ouyang, G.; McCann, J. T.; Xia, Y., Collecting electrospun nanofibers with patterned electrodes. *Nano Letters* **2005,** *5* (5), 913-916.

16. Yan, G.; Yu, J.; Qiu, Y.; Yi, X.; Lu, J.; Zhou, X.; Bai, X., Self-assembly of electrospun polymer nanofibers: A general phenomenon generating honeycomb-patterned nanofibrous structures. *Langmuir* **2011,** *27* (8), 4285-4289.

17. Xu, H.; Li, H.; Chang, J., Controlled drug release from a polymer matrix by patterned electrospun nanofibers with controllable hydrophobicity. *Journal of Materials Chemistry B* **2013,** *1* (33), 4182-4188.

18. Li, H.; Xu, Y.; Xu, H.; Chang, J., Electrospun membranes: control of the structure and structure related applications in tissue regeneration and drug delivery. *Journal of Materials Chemistry B* **2014,** *2* (34), 5492-5510.

19. Cui, W.; Zhou, Y.; Chang, J., Electrospun nanofibrous materials for tissue engineering and drug delivery. *Science and Technology of Advanced Materials* **2016**, *11* (1) 014108.

20. Kakunuri, M.; Wanasekara, N. D.; Sharma, C. S.; Khandelwal, M.; Eichhorn, S. J., Three-dimensional electrospun micropatterned cellulose acetate nanofiber surfaces with tunable wettability. *Journal of Applied Polymer Science* **2017,** *134* (15) 44709.

21. Yu, D.-G.; Li, X.-Y.; Wang, X.; Chian, W.; Liao, Y.-Z.; Li, Y., Zero-order drug release cellulose acetate nanofibers prepared using coaxial electrospinning. *Cellulose* **2013,** *20* (1), 379-389.

22. Agnihotri, S. M.; Vavia, P. R., Diclofenac-loaded biopolymeric nanosuspensions for ophthalmic application. *Nanomedicine: Nanotechnology, Biology and Medicine* **2009,** *5* (1), 90-95.

23. Shen, X.; Yu, D.; Zhu, L.; Branford-White, C.; White, K.; Chatterton, N. P., Electrospun diclofenac sodium loaded Eudragit® L 100-55 nanofibers for colon-targeted drug delivery. *International Journal of Pharmaceutics* **2011,** *408* (1), 200-207.

24. Khatri, Z.; Arain, R. A.; Jatoi, A. W.; Mayakrishnan, G.; Wei, K.; Kim, I.-S., Dyeing and characterization of cellulose nanofibers to improve color yields by dual padding method. *Cellulose* **2013,** *20* (3), 1469-1476.

25. Yohe, S. T.; Herrera, V. L.; Colson, Y. L.; Grinstaff, M. W., 3D superhydrophobic electrospun meshes as reinforcement materials for sustained local drug delivery against colorectal cancer cells. *Journal of Controlled Release* **2012,** *162* (1), 92-101.

26. Costa, P.; Lobo, J. M. S., Modeling and comparison of dissolution profiles. *European journal of pharmaceutical sciences* **2001,** *13* (2), 123-133

27. Arifin, D. Y.; Lee, L. Y.; Wang, C.-H., Mathematical modeling and simulation of drug release from microspheres: Implications to drug delivery systems. *Advanced drug delivery reviews* **2006,** *58* (12), 1274-1325.

28. Shen, X.; Yu, D.; Zhu, L.; Branford-White, C.; White, K.; Chatterton, N. P., Electrospun diclofenac sodium loaded Eudragit® L 100-55 nanofibers for colon-targeted drug delivery. *International journal of pharmaceutics* **2011,** *408* (1), 200-207.

29. Taepaiboon, P.; Rungsardthong, U.; Supaphol, P., Drug-loaded electrospun mats of poly (vinyl alcohol) fibres and their release characteristics of four model drugs. *Nanotechnology* **2006,** *17* (9), 2317.

30. Jannesari, M.; Varshosaz, J.; Morshed, M.; Zamani, M., Composite poly (vinyl alcohol)/poly (vinyl acetate) electrospun nanofibrous mats as a novel wound dressing matrix for controlled release of drugs. *Int J Nanomedicine* **2011,** *6*, 993-1003.

31. Piras, A.; Nikkola, L.; Chiellini, F.; Ashammakhi, N.; Chiellini, E., Development of diclofenac sodium releasing bio-erodible polymeric nanomats. *Journal of nanoscience and nanotechnology* **2006,** *6* (9-1), 3310-3320.

32. Nikkola, L.; Seppälä, J.; Harlin, A.; Ndreu, A.; Ashammakhi, N., Electrospun multifunctional diclofenac sodium releasing nanoscaffold. *Journal of nanoscience and nanotechnology* **2006,** *6* (9-1), 3290-3295.

33. Taepaiboon, P.; Rungsardthong, U.; Supaphol, P., Effect of cross-linking on properties and release characteristics of sodium salicylate-loaded electrospun poly (vinyl alcohol) fibre mats. *Nanotechnology* **2007,** *18* (17), 175102.